Journal of Materiomics 11 (2025) 101044

Contents lists available at ScienceDirect

Journal of Materiomics

journal homepage: www.journals.elsevier.com/journal-of-materiomics/

Research paper

# Thermal stability of FeSi as barrier layer in high-performance $Mg_2Si_{0.3}Sn_{0.7}$ thermoelectric device

Shanshan Hu [a, 1], Chen Huang [b, 1], Changyuan Li [a], Long Yang [a], Zhiwei Chen [a], Baisheng Sa [b, *], Wen Li [a, **], Yanzhong Pei [a, ***]

[a] Interdisciplinary Materials Research Center, School of Materials Science and Engineering, Tongji University, 4800 Caoan Road, Shanghai, 201804, China
[b] College of Materials Science and Engineering, Fuzhou University, 2 North Wulongjiang Road, Fuzhou, 350108, China

ARTICLE INFO

*Article history:*
Received 9 November 2024
Received in revised form
10 December 2024
Accepted 16 December 2024
Available online 14 March 2025

ABSTRACT

Thermal stability of thermoelectric devices plays a pivotal role in their practical applications. Chemical reaction/diffusion between thermoelectric materials and electrodes is one of the primary factors contributing to the degradation/failure of device performance at elevated temperatures. Introducing barrier layers to impede the behavior of chemical reactions has emerged as an effective approach for averting the failure of these devices. In this work, the FeSi is revealed to be a potent material of barrier layer in high-performance $Mg_2Si_{0.3}Sn_{0.7}$ thermoelectric material based on the considerations of interfacial reaction energy and sinterability. The well-established bond in $Mg_2Si_{0.3}Sn_{0.7}$/FeSi joint results in a low contact resistivity of ~20 $\mu\Omega\cdot cm^2$ and a conversion efficient of ~6.5% for the $Mg_2Si_{0.3}Sn_{0.7}$ single-leg device is achieved at a temperature difference of ~290 K. Long-term measurements of the device at a hot-side temperature of 600 K reveal that the performance remains nearly invariable as time further increases, which suggests that the FeSi layer retards the chemical reaction/diffusion.


## 1. Introduction

The majority of energy production and conversion processes are based on thermal engineering, which often results in significant carbon emissions. In the pursuit of sustainable development and carbon neutrality, thermoelectric generators with their advantages of zero emissions and silent operation, stand out as a highly promising green technology [1–3]. The efficiency and power output of the generators are contingent upon the performance of thermoelectric materials, which is determined by the dimensionless figure of merit $zT = S^2T/\rho(\kappa_E+\kappa_L)$ and the power factor $PF=S^2/\rho$, respectively ($S$, $\rho$, $T$, $\kappa_E$ and $\kappa_L$ are the Seebeck coefficient, electrical resistivity, absolute temperature, electronic and thermal conductivities, respectively) [4,5].

So far research efforts concerning materials have primarily focused on enhancing the performance of existing thermoelectric materials and uncovering high-performance novel thermoelectric candidates. Band convergence, which involves increasing the band degeneracy ($N_v$), has emerged as a prominent strategy for enhancing both PF and $zT$, enabling breakthroughs in a variety of thermoelectric materials, including PbTe [6], GeTe [7], SnTe [8], SnSe [9], $CoSb_3$ [10], $(Bi,Sb)_2Te_3$ [11], $Mg_2(Si,Sn)$ [12], half-Heusler [13] and Zintl phases [14]. Alternatively, the introduction of diverse defects to further scatter phonons and thereby reducing $\kappa_L$ [15–17], acts as an indispensable pathway for maximizing the $zT$. Furthermore, the features of complex crystal structure, soft chemical bonding and intrinsic vacancy generally accompany with an inherently low $\kappa_L$. These characteristics serve as a guiding principle for exploring novel high-performance thermoelectric materials, such as argyrodite compounds [18,19], $Cu_2SnSe_4$ [20,21] and $Ag_5Te_3$ [22].

Advancements in material performance have increased the demand for fabricating efficient and sustainable thermoelectric devices. Interfacial contacts between thermoelectric materials and electrodes, characterized by low electrical conductivity, high thermal conductivity, strong bonding and thermal stability, play as a critical role in determining the durability of the devices [23–25]. Note that the typical weldable electrodes of Cu and Ag, usually being the efficient dopants in many thermoelectric materials, are reactive to form internal compounds at elevated temperatures and

* Corresponding author.
** Corresponding author.
*** Corresponding author.
*E-mail addresses:* bssa@fzu.edu.cn (B. Sa), liwen@tongji.edu.cn (W. Li), yanzhong@tongji.edu.cn (Y. Pei).
[1] These authors contributed equally.

https://doi.org/10.1016/j.jmat.2025.101044

thereby result in the invalidation of the devices [26–29]. The implementation of barrier layers has been extensively showcased as a proficient means to hinder chemical diffusion/reaction at the interfaces [30].

$Mg_2Si$ has attracted widespread attention in the field of thermoelectric applications owning to its low density, non-toxicity, elemental abundance and exceptional thermoelectric performance [31,32]. The controllable manipulation of the conduction band through $Mg_2Sn$ alloying facilitates an PF of ~42 μW/(cm·K$^2$) and an average $zT_{ave.}$ of ~1.03 within 300–675 K for $Mg_2Si_{0.3}Sn_{0.7}$ alloy with the additional help of $\kappa_L$-reduction [33]. These results ensure the achievement of high power output and conversion efficiency for the devices. However, establishing a robust interfacial contact remains a significant challenge due to the pronounced chemical reactivity of Mg and Si elements towards the electrode materials including Cu, Ag and Ni [34–36]. Hence, the quest for a suitable barrier layer that exhibits inertness to both thermoelectric materials and the electrodes, becomes an urgent concern that needs to be addressed immediately.

In this work, transition metal silicides exhibiting metallic conduction behavior are proposed as potential barrier materials. The positive values for the interfacial reaction energy indicate their inertness towards high-performance $Mg_2Si_{0.3}Sn_{0.7}$ thermoelectric material, thereby theoretically demonstrating the chemical stability of the interfaces. Further considering the sinterability, a well-bonding $Mg_2Si_{0.3}Sn_{0.7}$/FeSi joint with a low contact resistivity of ~20 μΩ·cm$^2$ is obtained, even though a small amount of Mg diffusion in FeSi is observed. As a result, a conversion efficiency of 6.5% was realized for the $Mg_2Si_{0.3}Sn_{0.7}$ single-leg device at a temperature difference of ~290 K.

## 2. Experimental section

Polycrystalline $Mg_{2.03}(Si_{0.3}Sn_{0.7})_{0.993}Bi_{0.007}$ samples were synthesized by melting stoichiometric high-purity (>99.99%) elements (Mg, Si, Sn and Bi) in sealed tantalum tubes in quartz ampoules at 1330 K for 7 h, followed by quenching in cold water and annealing at 973 K for 72 h. The resulting ingots were manually ground into fine powders for phase composition analysis using X-ray diffraction (XRD) and pellet preparation through hot-pressing. Dense pellets (>98%) with a diameter of ~12 mm were sintered for transport property measurements by hot pressing at 973 K for 60 min under a uniaxial pressure of ~110 MPa.

Transport properties of the Hall coefficient ($R_H$), resistivity ($\rho$) and Seebeck coefficient ($S$) were simultaneously measured under helium (He) atmosphere. The $R_H$ and $\rho$ were measured using the Van der Pauw method. The $S$ was determined from the slope of thermopower versus temperature difference within the range of 0–5 K. Thermal diffusivity ($D$) was measured using the laser flash technique, and thermal conductivity ($\kappa$) was determined by $\kappa = dC_pD$, where $d$ is the density measured using the mass and geometric volume and the specific heat ($C_p$) was measured using a differential scanning calorimetry (DSC). The measurement uncertainties of $R_H$, $\rho$, $S$ and $D$ were about 5%.

FeSi ingots were synthesized by the arc melting of stoichiometric high-purity (>99.99%) elements (Fe and Si), which were then ground into powders using a high-energy ball mill at 500 r/min for 12 h. The bulks of Cu/FeSi/$Mg_{2.03}(Si_{0.3}Sn_{0.7})_{0.993}Bi_{0.007}$/FeSi/Cu were fabricated by one-step hot pressing using powders of FeSi, Cu and $Mg_{2.03}(Si_{0.3}Sn_{0.7})_{0.993}Bi_{0.007}$. The process was performed at a temperature of 933 K under a uniaxial pressure of ~110 MPa for 60 min. The bulks were then cut into the legs with size of ~1.3 mm × 1.3 mm × 5.5 mm for the measurements of interfacial contact resistance ($R_c$) and efficiency ($\eta$), and the estimation of thermal stability after aging at 550 K for different times.

The $R_c$ was measured using the four-probe technique. The $\eta$ of the single-leg devices was measured by a home-made efficiency system, where the legs were loaded between the heater and the heat-flow meter using liquid metals. Two K-type thermocouples, labeled as $T_1$ and $T_2$, were embedded at two sides of the leg to measure both the temperature difference and the output voltage. The copper bar (cross-sectional area of 3 mm × 3 mm) was used as a heat-flow meter and two K-type thermocouples ($T_3$ and $T_4$) with a small diameter of 0.06 mm were embedded to determine the temperature difference. The output current was measured through the metal heater block and heat-flow meter.

Microstructures and compositions were analyzed using a scanning electron microscope (SEM) equipped with an energy dispersive spectrometer (EDS). Optical reflectance was measured by a Fourier transform infrared spectrometer equipped with a diffuse reflectance attachment. Samples with the size of 2.5 mm × 1.0 mm × 10.0 mm, 3 mm × 3 mm × 6 mm were used for three-point bending and compressive tests by a micro-computer controlled electronic universal test machine with a loading rate of 0.03 mm/min and 0.5 mm/min, respectively.

## 3. Results and discussions

Thermoelectric technique as a sustainable remedy for the energy crisis and environmental issues, proposes the demand for low cost and eco-friendly thermoelectric materials. Non-toxic $Mg_2Si_{0.3}Sn_{0.7}$ not only possesses exceptional thermoelectric performance [37], but also boasts the most cost-effective nature among the existing n-type thermoelectric materials [38] (Fig. 1a). Moreover, this compound exhibits mechanical properties comparable to those of the renowned high-performance thermoelectric materials [39–45], as shown in Fig. 1b and Fig. S1. All these results prompt this work to be dedicated to search for effective barrier materials to promote practical applications of $Mg_2Si_{0.3}Sn_{0.7}$-based thermoelectric devices.

The XRD pattern of $Mg_{2.03}(Si_{0.3}Sn_{0.7})_{0.993}Bi_{0.007}$ is shown in Fig. S2a, suggesting the formation of a single phase. This is further confirmed by the absence of impurities and the homogeneous elemental distribution as revealed by SEM observation and the corresponding EDS analysis (Fig. S2c). The optical band gap ($E_g$) for the obtained material is estimated to be ~0.41 eV (Fig. S2b), which is in well agreement with the literature result (~0.46 eV)[33].

The transport properties for $Mg_{2.03}(Si_{0.3}Sn_{0.7})_{0.993}Bi_{0.007}$ are shown in Fig. 2. The obtained sample in this work displays a Hall carrier concentration ($n_H$) of ~1.4 × 10$^{20}$ cm$^3$, approaching its maximum [33], and a Hall mobility ($\mu_H$) of ~60 cm$^2$/(V·s) (Fig. 2a). As shown in Fig. 2b, the increases in both resistivity and Seebeck coefficient with increasing temperature illustrate the degenerate conduction behavior, which is in accordance with the Hall measurement results. The total thermal conductivity ($\kappa$, Fig. 2c) is calculated using the measured $C_p$ (Fig. S3a). The determination of $\kappa_L$ entails subtracting the electronic contribution ($\kappa_E$), which is dictated by the Wiedemann-Franz law ($\kappa_E = LT/\rho$), from the overall thermal conductivity ($\kappa$) (Fig. 2c). Here, the Lorentz factor ($L$) is ascertained using the single parabolic band (SPB) model, with acoustic phonon scattering being taken into account. As a result, a PF higher than ~37 μW/(cm·K$^2$) and a peak $zT$ of ~1.0 are attained here. All the transport properties are comparable to those of the reported $Mg_2Si_{0.7}Sn_{0.3}$-based thermoelectric material with a similar $n_H$ [33]. Moreover, the repeated measurements elucidate the stability of the material when the temperature is lower than 600 K. When further compared to the n-type thermoelectric materials with high-performance in the temperature range of 300–600 K (Fig. 3), the $Mg_2Si_{0.7}Sn_{0.3}$ exhibits a leading $PF_{ave}$, ensuring superior power output of the related thermoelectric

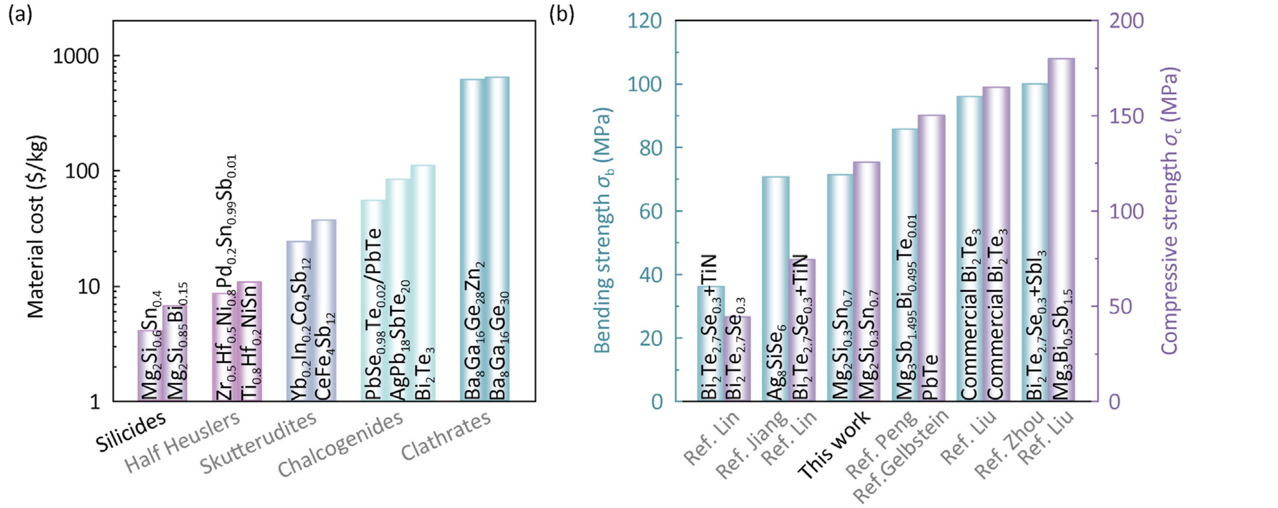


**Fig. 1.** Cost [38] (a) and mechanical properties [39–45] (b) for $Mg_{2.03}(Si_{0.3}Sn_{0.7})_{0.993}Bi_{0.007}$ with a comparison to those of ever-reported n-type thermoelectric materials.

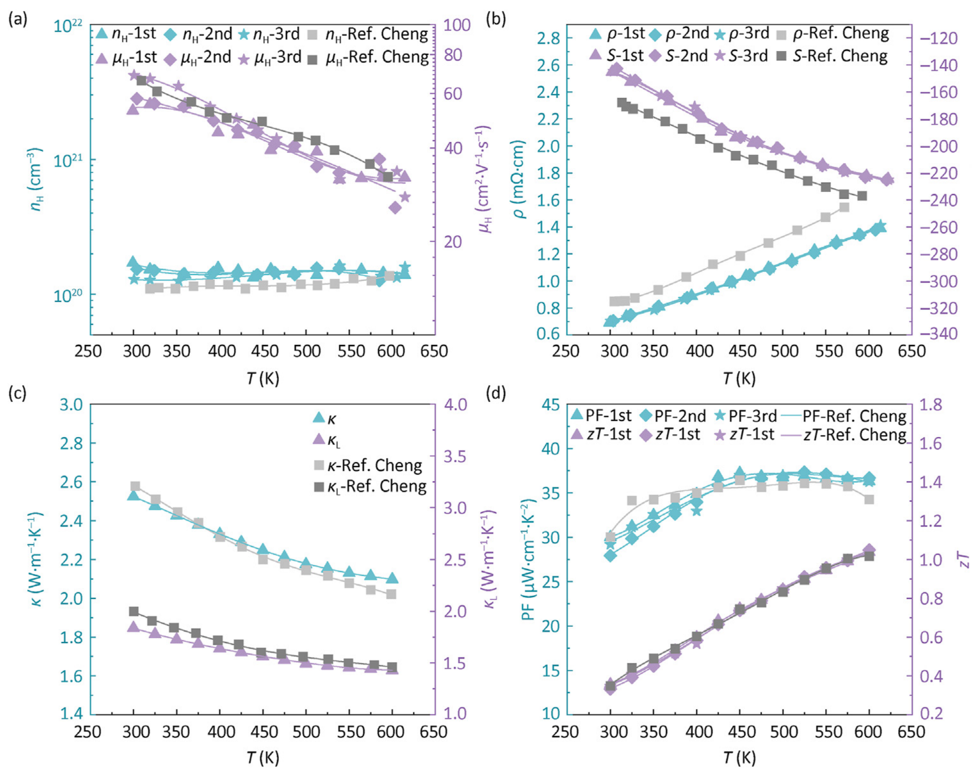


**Fig. 2.** Temperature dependent Hall carrier concentration ($n_H$) and Hall mobility ($\mu_H$) (a), resistivity ($\rho$) and Seebeck coefficient ($S$) (b), total ($\kappa$) and lattice ($\kappa_L$) thermal conductivities (c) and power factor (PF) and figure of merit ($zT$) (d) for $Mg_{2.03}(Si_{0.3}Sn_{0.7})_{0.993}Bi_{0.007}$ with a comparison to those of literatures [33].

devices. However, its average $zT_{ave}$ is found to be lower than that of $AgSbTe_2$- [1,55], $Mg_3(Sb, Bi)_2$- [46–51], $Bi_2Te_3$- [53], and PbTe-based [54] thermoelectric materials.

In addition to the superior thermoelectric performance, the robust interfacial contact also acts as a crucial factor in determining the performance and durability of the devices. Owing to the chemical activity of Mg and Si, the transition metal silicides including MnSi, FeSi, CoSi and NiSi that exhibit metallic conduction behavior are considered as potential barrier materials here. The interfacial reaction energy ($E_{IR}$) between $Mg_2Si$/$Mg_2Sn$ and these silicides is calculated based on their formation energy at 0 K, which is obtained by the first-principles calculations (Tables S1–S2). The formation energy at 0 K serves as a straightforward and rapid indication on the reactivity of the considered compounds, but the calculation of Gibbs free energy needs to be done for accurate predictions. As shown in Fig. 4a, the positive values of the calculated reaction energy suggest the inertness of the barrier materials with respect to $Mg_2Si$ and $Mg_2Sn$. The formation energy between FeSi and $Mg_2Sn$ exhibits the highest positive value, indicating that FeSi can be prioritized as the barrier layer for device preparation

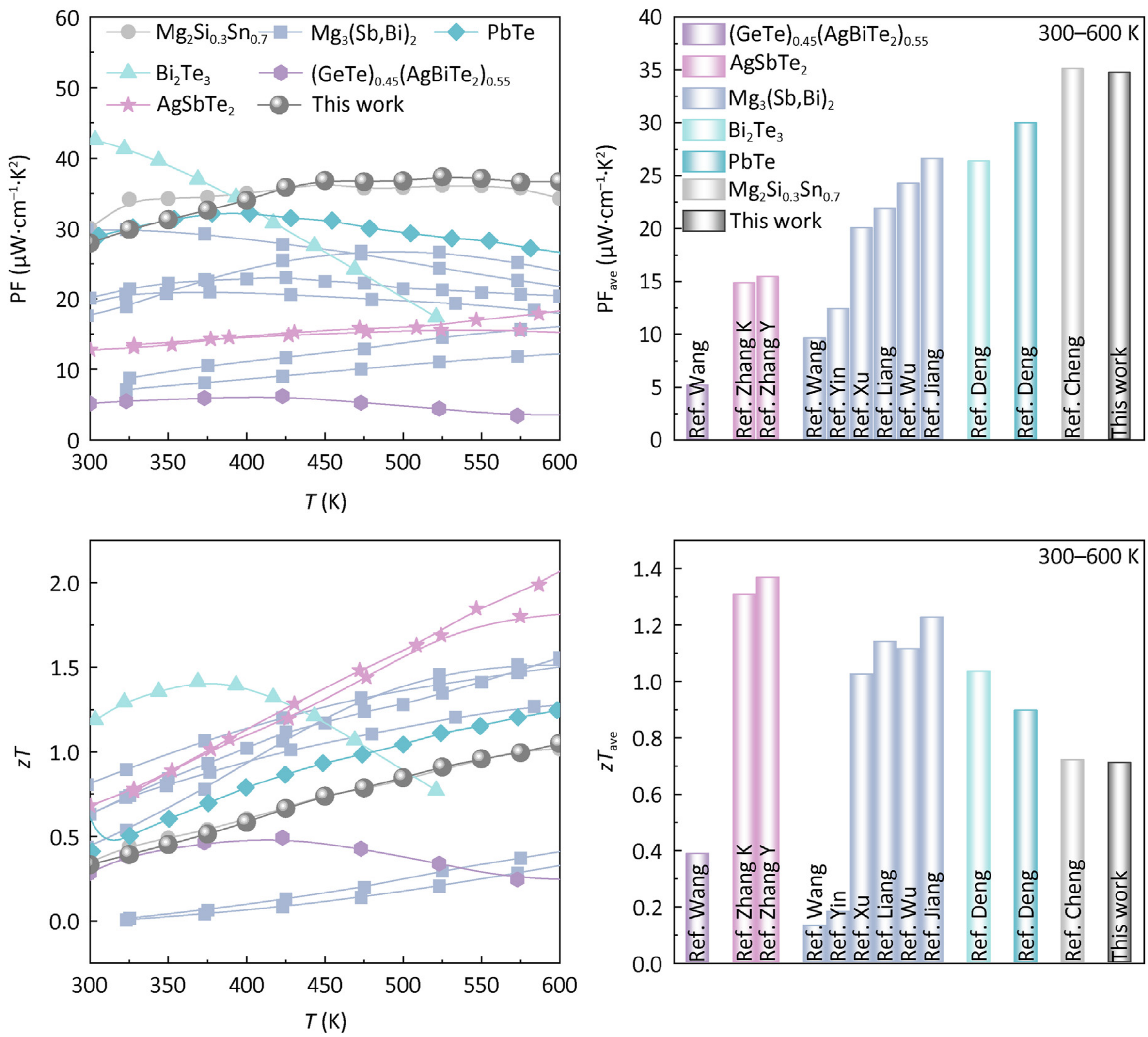


**Fig. 3.** Comparison of temperature-dependent and average PF (a, b) and $zT$ (c, d) for $Mg_{2.03}(Si_{0.3}Sn_{0.7})_{0.993}Bi_{0.007}$ to those of the ever-reported n-type thermoelectric materials [1,33,46–55].

and research. For FeSi, the formation energy and the Gibbs free energy are both positive due to the negative entropy difference, thus inertness at all temperatures is expected. Additionally, under suitable fabrication conditions, other silicides may also serve as potential barrier layers for further investigation.

The strong bonds that facilitate excellent electrical and thermal conductivity between thermoelectric material and electrode is imperative for the thermoelectric devices. The successful fabrication of $Cu/FeSi/Mg_{2.03}(Si_{0.3}Sn_{0.7})_{0.993}Bi_{0.007}$ bulks *via* one-step hot pressing further drives the current work to concentrate on the thermal stability of FeSi (Fig. S3b) as the barrier layer. The schematic of the bulk preparation is shown in Fig. S4a. The legs with a size of 1.3 mm × 1.3 mm × 5.5 mm are cut from the bulks for interface characterization, and interfacial contact resistance and conversion efficiency measurements. The specific interfaces are characterized by the SEM observation and EDS analysis, as shown in Fig. 4b. The boundaries without voids illustrate the well-established bonding of Cu/FeSi and $Mg_{2.03}(Si_{0.3}Sn_{0.7})_{0.993}Bi_{0.007}$/FeSi joints. The chemical inertness is reliably demonstrated by the impeded diffusion or reaction. The aging of the legs is carried out at 550 K to further identify the element diffusions. The SEM observations (Fig. S5) qualitatively verify that the introduction of FeSi barrier layer remains a passivation strategy for extending the service life of the $Mg_{2.03}(Si_{0.3}Sn_{0.7})$-based device. The electrical contact resistance ($R_c$) for the joint is measured by a four-probe technique and the measurement schematic is shown in the inset of Fig. 4c. The $R_c$ is found to be 1.16 mΩ and 1.67 mΩ at both ends of the leg, which correspond to the electrical contact resistivities ($\rho_c$) of 19.6 μΩ·cm$^2$ and 28.2 μΩ·cm$^2$, respectively. The obtained $\rho_c$ is found to be lower than that of $Mg_2Cu$ barrier material [33], which firmly reveals FeSi as a promising barrier candidate for $Mg_{2.03}(Si_{0.3}Sn_{0.7})_{0.993}Bi_{0.007}$ thermoelectric.

The single-leg device with a size of 1.3 mm × 1.3 mm × 5.5 mm is utilized for measuring the power output ($P$) and efficiency ($\eta$). Schematic of the measurement is shown in Fig. S4b and the corresponding results are shown in Fig. 5. The cold side temperature is fixed at 300 K to measure the performance of the devices. The output voltage ($V$) versus current ($I$) for $Mg_{2.03}(Si_{0.3}Sn_{0.7})_{0.993}Bi_{0.007}$ single-leg device with FeSi barrier layers and Cu electrodes under different $\Delta T$ is shown in Fig. 5a. The open circuit voltage ($V_{oc}$) and the internal resistance ($R_{in}$) can be determined by the intercepts and slopes of the linearly fitted $V$–$I$ curves, respectively. The rise in

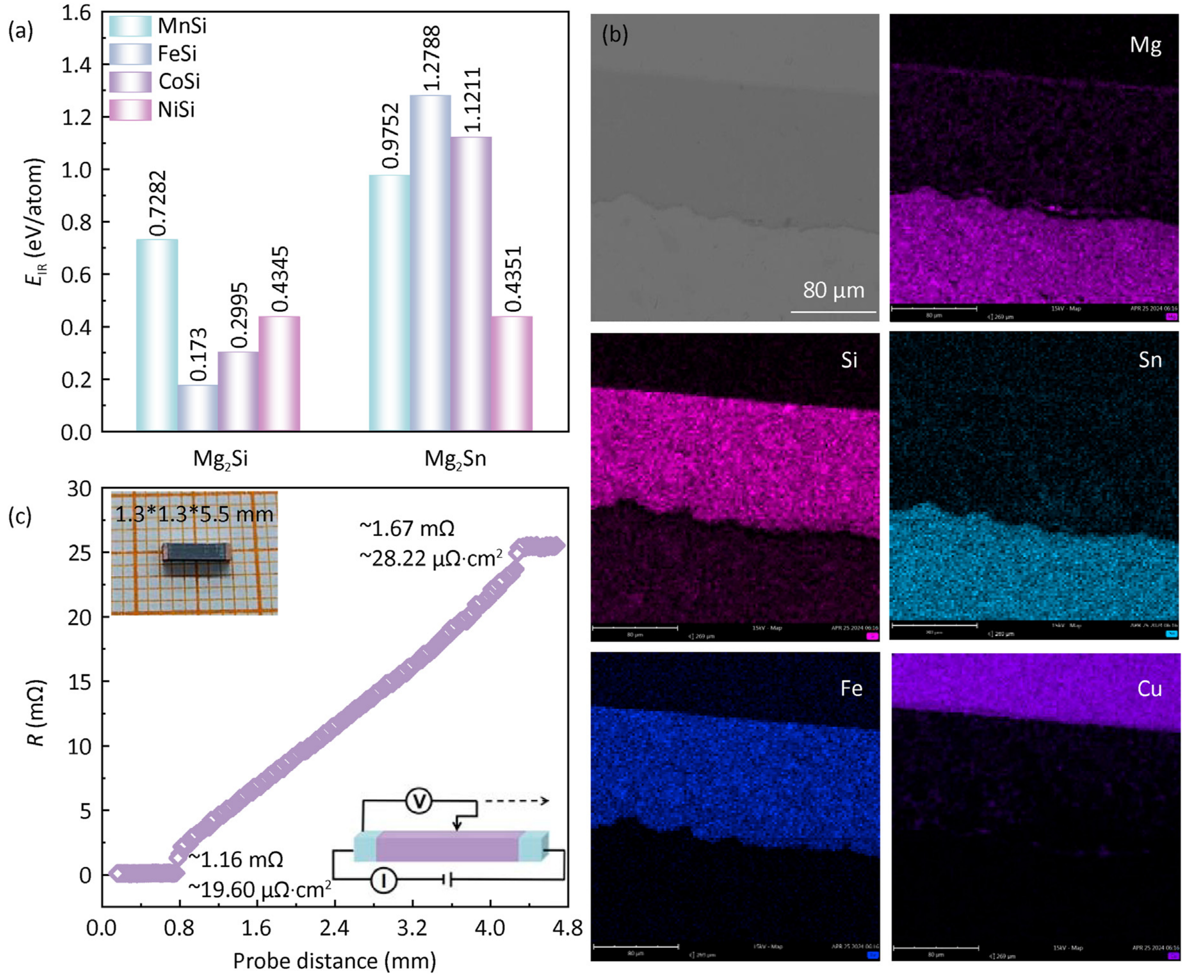


**Fig. 4.** Calculated interfacial reaction energy ($E_{IR}$) for $Mg_2Si$ and $Mg_2Sn$ thermoelectrics with the potential barrier materials (a). SEM image and corresponding EDS mapping (b) and room temperature interfacial contact resistance measured using a line scanning technique (c) for $Mg_{2.03}(Si_{0.3}Sn_{0.7})_{0.993}Bi_{0.007}$/FeSi/Cu joint.

$V_{oc}$ with increasing $\Delta T$ is attributed to the increased Seebeck coefficient at elevated temperatures. Moreover, the measured $V_{oc}$ is close to the prediction based on the temperature-dependent Seebeck coefficient of thermoelectric material, as shown in Fig. S6a. While the $R_{in}$ is found to be larger than that predicted using the material's resistivity (Fig. S6b), this discrepancy stems from the presence of interfacial contact resistance.

The $V_{oc}$, $P$, and $\eta$ under different temperature gradients ($\Delta T$) are presented in Fig. 5a–c, respectively. A $P$ of up to 28 mW is achieved at a $\Delta T$ of ~290 K (Fig. 5b), which corresponds to a power density ($P_d$) of 1.65 W/cm$^2$. Moreover, a conversion efficiency $\eta$ of ~6.5% is realized under $\Delta T = 290$ K (Fig. 5c). Since the $R_{in}$ for the single-leg device is smaller than the minimal $R_{load}$ of the measurement system, the measured $P$ and $\eta$ are lower than their maximum in this work, where the maximum $P_{max}$ of 36.5 mW and $\eta_{max}$ of 7.9% are obtained through the extrapolation based on the measured results at each temperature gradient (Fig. 5b–c). The $P_{max}$ and $\eta_{max}$ extrapolated from the measured data are in agreement with the predictions based on the measured material and interface properties (Figs. S6c and S6d, where $R_c$ is about 2.83 mΩ). The predicted maximal $P_d$ (Fig. 5d) and $\eta_{max}$ for $Mg_{2.03}(Si_{0.3}Sn_{0.7})_{0.993}Bi_{0.007}$ single-leg device in this work ranks the highest among the reported n-type thermoelectric single-leg devices at temperature below 600 K, while the predicted $\eta_{max}$ (Fig. 5e) is slight lower that of them. These findings underline the potential of this material as a prominent n-type component for the thermoelectric generators to harness low-grade heat.

Meanwhile, an initial deterioration of $\eta_{max}$ and $P_{max}$ is observed during the long-term stability measurements at a hot-side temperature of 600 K as shown in Fig. 5f. The performance degradation can be attributed to the loss of Mg and Sn as well as the trace diffusion of Cu [34] due to the limited effectiveness of the FeSi barrier layer, leading to increased resistances at the interface and within the thermoelectric material. Consequently, optimizing the interface between the electrode and the $Mg_2$(Si, Sn)-based thermoelectric material to enhance its thermal stability warrants further investigation.

The long-term measurements for the single-leg device are conducted at a hot-side temperature of 600 K to illustrate the thermal stability, and the corresponding results are shown in Fig. 5f. The deteriorations in $\eta_{max}$ and $P_{max}$ are observed initially for the single-leg device measured at 600 K, which then remain nearly constant. The degraded performance was associated with to Mg and Sn loss as well as trace Cu diffuse [34], leading to the increased resistances of interface and thermoelectric material. Therefore, the optimization of the interface between electrodes and $Mg_2$(Si, Sn)-based thermoelectric materials so as to enhance their thermal stability merits further exploration.

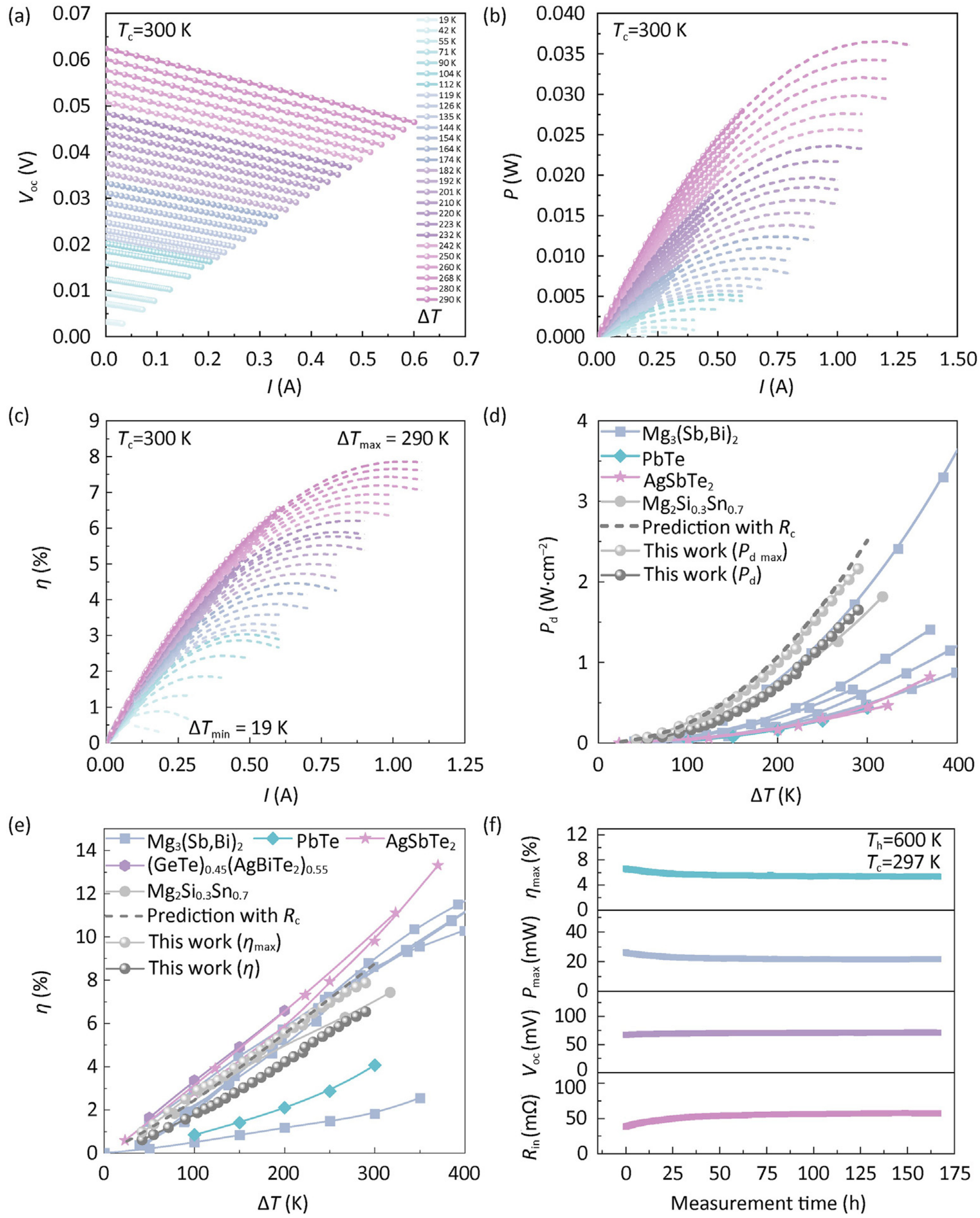


**Fig. 5.** Output voltage (a), output power (b) and conversion efficiency (c) versus current (the solid lines are the measured curves, and the dashed lines are the extrapolated curves), power density (d) and maximum conversion efficiency (e) *versus* temperature-difference for $Mg_{2.03}(Si_{0.3}Sn_{0.7})_{0.993}Bi_{0.007}$ single-leg device with a comparison to the prediction and the literature results [1,33,46–55]. Maximum efficiency ($\eta_{max}$), maximum output power ($P_{max}$), open circuit voltage ($V_{oc}$) and internal resistance ($R_{in}$) for the device during the long-term measurements at the hot side temperature of 600 K (f).

## 4. Conclusions

In summary, based on the calculated interfacial reaction energy and sinterability, FeSi is proposed as a potential barrier candidate for $Mg_{2.03}(Si_{0.3}Sn_{0.7})_{0.993}Bi_{0.007}$ thermoelectric material. The firmly established bonding between the barrier layer and the thermoelectric material facilitates a low contact resistivity of ~20 μΩ·cm$^2$, enabling a superior power output of ~28 mW and an exceptional conversion efficiency of 6.5% at a temperature difference of 290 K. Although trace diffusions of Mg, Sn and Cu are observed, the device performance remains nearly constant as time increase for the long-term measurements at a hot-side temperature of 600 K, which indicates that the FeSi layer retards the chemical reaction/diffusion in $Mg_{2.03}(Si_{0.3}Sn_{0.7})_{0.993}Bi_{0.007}$ single-leg device.

## CRediT authorship contribution statement

**Shanshan Hu:** Writing – original draft, Investigation. **Chen Huang:** Software, Data curation. **Changyuan Li:** Software, Methodology. **Long Yang:** Methodology. **Zhiwei Chen:** Formal analysis. **Baisheng Sa:** Formal analysis. **Wen Li:** Writing – review & editing, Supervision. **Yanzhong Pei:** Supervision, Conceptualization.

## Declaration of competing interest

The authors declare that they have no known competing financial interests or personal relationships that could have appeared to influence the work reported in this paper.

## Acknowledgments

This work was supported by the National Key Research and Development Program of China (2023YFB3809400), the National Natural Science Foundation of China (Grant Nos. T2125008, 92163203 and 52371234), the Innovation Program of Shanghai Municipal Education Commission (202101-07-00-07-E00096), the Hong Kong, Macao and Taiwan Science and Technology Cooperation Project for Science and Technology Innovation Plan of Shanghai (23520760600) and the Fundamental Research Funds for the Central Universities.

## Appendix A. Supplementary data

Supplementary data to this article can be found online at https://doi.org/10.1016/j.jmat.2025.101044.

## References

[1] Zhang K, Liu S, Wang X, Wu S, Xiong Q, Wang X, et al. Dual alloying enables high thermoelectric performance in $AgSbTe_2$ by manipulating carrier transport behavior. Adv Funct Mater 2024;34:2400679.
[2] Wang L, Zhang W, Back SY, Kawamoto N, Nguyen DH, Mori T. High-performance $Mg_3Sb_2$-based thermoelectrics with reduced structural disorder and microstructure evolution. Nat Commun 2024;15:6800.
[3] Sun C, Shi X, Zheng L, Chen B, Li W. Transport properties of p-type $CaMg_2Bi_2$ thermoelectrics. J Materiomics 2019;5:567–73.
[4] Wu R, Li Z, Li Y, You L, Luo P, Yang J, et al. Synergistic optimization of thermoelectric performance in p-type $Ag_2Te$ through Cu substitution. J Materiomics 2019;5:489–95.
[5] Song J, Luo P, Sun H, Li H, Wang C, Niu Y, et al. Bismuth-free $Mg_3Sb_2$ with enhanced room-temperature thermoelectric and mechanical properties. J Materiomics 2024;10:1101–8.
[6] Chen Z, Jian Z, Li W, Chang Y, Ge B, Hanus R, et al. Lattice dislocations enhancing thermoelectric PbTe in addition to band convergence. Adv Mater 2017;29:1606768.
[7] Li J, Zhang X, Chen Z, Lin S, Li W, Shen J, et al. Low-symmetry rhombohedral GeTe thermoelectrics. Joule 2018;2:976–87.
[8] Moshwan R, Yang L, Zou J, Chen Z-G. Eco-friendly SnTe thermoelectric materials: progress and future challenges. Adv Funct Mater 2017;27:1703278.
[9] Liu D, Wang D, Hong T, Wang Z, Wang Y, Qin Y, et al. Lattice plainification advances highly effective SnSe crystalline thermoelectrics. Science 2023;380: 841–6.
[10] Tang Y, Gibbs ZM, Agapito LA, Li G, Kim H-S, Nardelli MB, et al. Convergence of multi-valley bands as the electronic origin of high thermoelectric performance in $CoSb_3$ skutterudites. Nat Mater 2015;14:1223–8.
[11] Witting IT, Chasapis TC, Ricci F, Peters M, Heinz NA, Hautier G, et al. The Thermoelectric properties of bismuth telluride. Adv Electron Mater 2019;5: 1800904.
[12] Mao J, Wang Y, Ge B, Jie Q, Liu Z, Saparamadu U, et al. Thermoelectric performance enhancement of $Mg_2Sn$ based solid solutions by band convergence and phonon scattering *via* Pb and Si/Ge substitution for Sn. Phys Chem Chem Phys 2016;18:20726–37.
[13] Fu C, Zhu T, Liu Y, Xie H, Zhao X. Band engineering of high performance p-type FeNbSb based half-Heusler thermoelectric materials for figure of merit $zT$>1. Energy Environ Sci 2015;8:216–20.
[14] Ohno S, Imasato K, Anand S, Tamaki H, Kang SD, Gorai P, et al. Phase boundary mapping to obtain n-type $Mg_3Sb_2$-based thermoelectrics. Joule 2018;2: 141–54.
[15] Tan X, Liu G, Xu J, Tan X, Shao H, Hu H, et al. Thermoelectric properties of In-Hg co-doping in SnTe: energy band engineering. J Materiomics 2018;4:62–7.
[16] Han Z, Li J-W, Jiang F, Xia J, Zhang B-P, Li J-F, et al. Room-temperature thermoelectric materials: challenges and a new paradigm. J Materiomics 2022;8: 427–36.
[17] Liu K-J, Zhang Z-W, Chen C, Wei L-H, He H-L, Mao J, et al. Entropy engineering in $CaZn_2Sb_2$-$YbMg_2Sb_2$ Zintl alloys for enhanced thermoelectric performance. Rare Met 2022;41:2998–3004.
[18] Lin S, Li W, Pei Y. Thermally insulative thermoelectric argyrodites. Mater Today 2021;48:198–213.
[19] Jin M, Lin S, Li W, Chen Z, Li R, Wang X, et al. Fabrication and thermoelectric properties of single-crystal argyrodite $Ag_8SnSe_6$. Chem Mater 2019;31: 2603–10.
[20] Qu L, Yang C, Luo Y, Li C, Du Z, Cui J. Improved thermoelectric performance of $Cu_2SnSe_4$ by proper decoupling between electron and phonon through replacement of Sn with. Adv Eng Mater 2023;25:2201487.
[21] Li W, Lin S, Zhang X, Chen Z, Xu X, Pei Y. Thermoelectric properties of $Cu_2SnSe_4$ with intrinsic vacancy. Chem Mater 2016;28:6227–32.
[22] Zhang X, Chen Z, Lin S, Zhou B, Gao B, Pei Y. Promising thermoelectric $Ag_{5-\delta}Te_3$ with intrinsic low lattice thermal conductivity. ACS Energy Lett 2017;2: 2470–7.
[23] Liu W, Bai S. Thermoelectric interface materials: a perspective to the challenge of thermoelectric power generation module. J Materiomics 2019;5:321–36.
[24] Xie L, Ming C, Song Q, Wang C, Liao J, Wang L, et al. Lead-free and scalable GeTe-based thermoelectric module with an efficiency of 12%. Sci Adv 2023;9: eadg7919.
[25] Wu X, Han Z, Zhu Y, Deng B, Zhu K, Liu C, et al. A general design strategy for thermoelectric interface materials in n-type $Mg_3Sb_{1.5}Bi_{0.5}$ single leg used in TEGs. Acta Mater 2022;226:117616.
[26] Hsieh H-C, Wang C-H, Lan T-W, Lee T-H, Chen Y-Y, Chu H-S, et al. Joint properties enhancement for PbTe thermoelectric materials by addition of diffusion barrier. Mater Chem Phys 2020;246:122848.
[27] Shen L, Chen Y, Niu B, Liu Z, Qin J, Xie J. Optimization of interface materials between $Bi_2Te_3$-based films and Cu electrodes enables a high performance thin-film thermoelectric cooler. ACS Appl Mater Interfaces 2022;14: 21106–15.
[28] Li CC, Drymiotis F, Liao LL, Hung HT, Ke JH, Liu CK, et al. Interfacial reactions between PbTe-based thermoelectric materials and Cu and Ag bonding materials. J Mater Chem C 2015;3:10590–6.
[29] Lin YC, Lee KT, Hwang JD, Chu HS, Hsu CC, Chen SC, et al. Solid liquid interdiffusion bonding of $Zn_4Sb_3$ thermoelectric material with Cu electrode. J Electron Mater 2016;45:4935–42.
[30] El-Genk WS, Saber HH. High efficiency segmented thermoelectric unicouple for operation between 973 and 300 K. Energy Convers Manag 2003;44: 1069–88.
[31] Santos R, Yamini SA, Dou SX. Recent progress in magnesium-based thermoelectric materials. J Mater Chem A 2018;6:3328–41.
[32] Caballero-Calero O, Ares JR, Martin-Gonzalez M. Environmentally friendly thermoelectric materials: high performance from inorganic components with low toxicity and abundance in the earth. Adv Sustainable Syst 2021;5: 2100095.
[33] Cheng K, Bu Z, Tang J, Zhang X, Meng X, Li W, et al. Efficient $Mg_2Si_{0.3}Sn_{0.7}$ thermoelectrics demonstrated for recovering heat of about 600 K. Mater Today Phys 2022;28:100887.
[34] Ayachi S, Hernandez GC, Pham NH, Farahi N, Mueller E, de Boor J. Developing contacting solutions for $Mg_2Si_{1-x}Sn_x$-based thermoelectric generators: Cu and $Ni_{45}Cu_{55}$ as potential contacting electrodes. ACS Appl Mater Interfaces 2019;11:40769–80.
[35] Pham NH, Farahi N, Kamila H, Sankhla A, Ayachi S, Mueller E, et al. Ni and Ag electrodes for magnesium silicide based thermoelectric generators. Mater Today Phys 2019;11:97–105.
[36] Ayachi S, Deshpande R, Ponnusamy P, Park S, Chung J, Park S, et al. On the relevance of point defects for the selection of contacting electrodes: Ag as an example for $Mg_2(Si,Sn)$-based thermoelectric generators. Mater Today Phys 2021;20:100309.
[37] Liu W, Yin K, Zhang Q, Uher C, Tang X. Eco-friendly high-performance silicide thermoelectric materials. Natl Sci Rev 2017;4:611–26.
[38] LeBlanc S, Yee SK, Scullin ML, Dames C, Goodson KE. Material and manufacturing cost considerations for thermoelectrics. Renew Sustain Energy Rev 2014;32:313–27.
[39] Lin S, Li J, Yan H, Meng X, Xiang Q, Jing H, et al. Dramatically enhanced mechanical properties of nano-TiN-dispersed n-type bismuth telluride by multi-effect modulation. Materials 2024;17:1919.
[40] Jiang Q, Li S, Luo Y, Xin J, Li S, Li W, et al. Ecofriendly highly robust $Ag_8SiSe_6$-based thermoelectric composites with excellent performance near room temperature. ACS Appl Mater Interfaces 2020;12:54653–61.
[41] Peng X, Guo J, Su X, Wu J, Zhang Q, Tang X. Ultrafast combustion synthesis and high thermoelectric performance of $Mg_3Sb_{2-x}Bi_x$-based compounds. ACS Appl Energy Mater 2024;7:2552–60.
[42] Liu M, Zhang X, Zhang S, Pei Y. $Ag_2Se$ as a tougher alternative to n-type $Bi_2Te_3$ thermoelectrics. Nat Commun 2024;15:6580.
[43] Zhou J, Feng J, Li H, Liu D, Qiu G, Qiu F, et al. Modulation of vacancy defects and texture for high performance n-type $Bi_2Te_3$ *via* high energy refinement. Small 2023;19:2300654.
[44] Gelbstein Y, Gotesman G, Lishzinker Y, Dashevsky Z, Dariel MP. Mechanical properties of PbTe-based thermoelectric semiconductors. Scr Mater 2008;58: 251–4.
[45] Liu K, Chen C, Li X, Jia J, Xia C, Mao J, et al. Tuning the carrier scattering mechanism by rare-earth element doping for high average $zT$ in $Mg_3Sb_2$-based compounds. ACS Appl Mater Interfaces 2022;14:7022–9.
[46] Wu X, Lin Y, Han Z, Li H, Liu C, Wang Y, et al. Interface and surface engineering realized high efficiency of 13% and improved thermal stability in $Mg_3Sb_{1.5}Bi_{0.5}$-based thermoelectric generation devices. Adv Energy Mater 2022;12:2203039.
[47] Liang Z, Xu C, Shang H, Ning M, Tong T, Song S, et al. Near-Near-room-temperature thermoelectric performance enhancement *via* phonon spectra mismatch in $Mg_3(Sb,Bi)_2$-based material by incorporating multi-walled carbon nanotubes. Adv Energy Mater 2023;13:2301107.
[48] Jiang F, Wu X, Zhu Y, Xia C, Han Z, Yu H, et al. Boosting room-temperature thermoelectric performance of $Mg_3Sb_{1.5}Bi_{0.5}$ material through breaking the contradiction between carrier concentration and carrier mobility. Acta Mater 2024;265:119636.
[49] Xu C, Liang Z, Shang H, Wang D, Wang H, Ding F, et al. Scalable synthesis of n-type $Mg_3Sb_{2-x}Bi_x$ for thermoelectric applications. Mater Today Phys 2021;17: 100336.

[50] Yin L, Chen C, Zhang F, Li X, Bai F, Zhang Z, et al. Reliable N-type $Mg_{3.2}Sb_{1.5}Bi_{0.49}Te_{0.01}$/304 stainless steel junction for thermoelectric applications. Acta Mater 2020;198:25–34.
[51] Wang Y, Chen J, Jiang Y, Ferhat M, Ohno S, Munir ZA, et al. Suppression of interfacial diffusion in $Mg_3Sb_2$ thermoelectric materials through an $Mg_{4.3}Sb_3Ni/Mg_{3.2}Sb_2Y_{0.05}/Mg_{4.3}Sb_3Ni$-graded structure. ACS Appl Mater Interfaces 2022;14:33419–28.
[52] Wang D-Z, Liu W-D, Li M, Zheng K, Hu H, Yin L-C, et al. Hierarchical architectural structures induce high performance in n-type GeTe-based thermoelectrics. Adv Funct Mater 2023;33:2213040.
[53] Deng R, Su X, Hao S, Zheng Z, Zhang M, Xie H, et al. High thermoelectric performance in $Bi_{0.46}Sb_{1.54}Te_3$ nanostructured with ZnTe. Energy Environ Sci 2018;11:1520–35.
[54] Deng P-Y, Wang K-K, Sung H-Y, Wu W-W, Wu H-J. Liquid-like copper chalcogenide in high-performance n-type PbTe thermoelectrics. Cell Rep Phys Sci 2023;4:101413.
[55] Zhang Y, Li Z, Singh S, Nozariasbmarz A, Li W, Genc A, et al. Defect-engineering-stabilized $AgSbTe_2$ with high thermoelectric performance. Adv Mater 2023;35:2208994.

**Shanshan Hu** received her MS degree from South China Normal University, China. She is now a Ph.D. candidate at Tongji University under the supervision of Prof. Wen Li. Her research focuses on magnesium-based thermoelectric materials and thermoelectric biomaterials.

**Chen Huang** received her B.E. degree in material forming and control engineering from Hunan University of Science and Technology, China. She is now a postgraduate at Fuzhou University under the supervision of Prof. Baisheng Sa. Her research focuses on the automated workflow calculation of density functional theory for two-dimensional materials and optoelectronic device simulations.

**Baisheng Sa** holds a B.E. and a Ph.D. degree from Xiamen University. He is currently a professor at School of Materials Science and Engineering, Fuzhou University. His research interest is the integrated computational modelling, density functional theory calculations and machine learning design of novel functional materials for energy, environment, and electronic applications.

**Wen Li** has been working on the bottleneck problem of low conversion efficiency of current thermoelectric materials, devoted to designing and developing high-performance thermoelectric materials. He holds a B.E. and a M.S. degree from Zhengzhou University, a Ph.D. degree from Shizuoka University. He became an assistant researcher in 2013, an associate professor in 2017 and a professor in 2021 at the School of Materials Science and Engineering, Tongji University, Shanghai, China. His interests are focused on flexible thermoelectric materials and new biomedical materials.

**Yanzhong Pei** has been working on advanced thermoelectric semiconductors for longer than a decade, from synthesizing the materials to understanding the underlying physics and chemistry. He holds a B.E. degree from Central South University in China, a Ph.D. degree from Shanghai Institute of Ceramics, Chinese Academy of Sciences, and postdoctoral research experience for about five years at Michigan State University and the California Institute of Technology. He became a professor in 2012 at the School of Materials Science and Engineering, Tongji University, Shanghai, China. His interests are focused on materials physics and chemistry for energy applications.